Atmospheric
Chemistry
and Physics
Discussions

Airborne observations of trace gases over boreal Canada during BORTAS: campaign climatology, airmass analysis and enhancement ratios

S. J. O'Shea[1], G. Allen[1], M. W. Gallagher[1], S. J.-B. Bauguitte[2], S. M. Illingworth[1], M. Le Breton[1], J. B. A. Muller[1], C. J. Percival[1], A. T. Archibald[3], D. E. Oram[4], M. Parrington[5], P. I. Palmer[5], and A. C. Lewis[6]

[1]School of Earth, Atmospheric and Environmental Sciences, University of Manchester, Oxford Road, Manchester, M13 9PL, UK
[2]Facility for Airborne Atmospheric Measurements (FAAM), Building 125, Cranfield University, Cranfield, Bedford, MK43 0AL, UK
[3]Centre for Atmospheric Science, University of Cambridge, Cambridge CB2 1EW, UK
[4]National Centre for Atmospheric Science, School of Environmental Sciences, University of East Anglia, Norwich, NR4 7TJ, UK
[5]School of GeoSciences, The University of Edinburgh, Edinburgh, UK
[6]National Centre for Atmospheric Science (NCAS), University of York, Heslington, York YO10 5DD, UK

Title Page

Abstract	Introduction
Conclusions	References
Tables	Figures

|◀ | ▶|
◀ | ▶

Back | Close

Full Screen / Esc

Printer-friendly Version

Interactive Discussion

Correspondence to: S. J. O'Shea (sebastian.oshea@postgrad.manchester.ac.uk) and
G. Allen (grant.allen@manchester.ac.uk)

Abstract

In situ airborne measurements were made over Eastern Canada in summer 2011 as part of the BORTAS experiment (Quantifying the impact of BOReal forest fires on Tropospheric oxidants over the Atlantic using Aircraft and Satellites). In this paper we present observations of greenhouse gases (CO_2 and CH_4) and other biomass burning tracers and related trace gases, both climatologically and through case studies, as recorded on board the FAAM BAe-146 research aircraft. Vertical profiles of CO_2 were generally characterised by depleted boundary layer concentrations relative to the free troposphere, consistent with terrestrial biospheric uptake. In contrast, CH_4 concentrations were found to rise with decreasing altitude due to strong local and regional surface sources. We use coincident tracer-tracer correlations and a Lagrangian trajectory model to characterise and differentiate air mass history of intercepted plumes. In particular, CO, HCN and CH_3CN were used to identify air masses that have been recently influenced by biomass burning. Concentrations of CO_2 were found to have a mean tropospheric, campaign-average concentration of 384.8 ppm (ranging between 371.5 and 397.1 ppm), whilst CH_4 concentrations had a mean value of 1859 ppb (ranging between 1797 and 1968 ppb), representing the episodic sampling of local fire plumes. CH_4 and CO_2 concentrations during BORTAS were found to be broadly comparable to previous measurements in the region during the regional burning season and with reanalysed composition fields from the EU Monitoring Atmospheric Composition and Change (MACC) project. By examining individual case studies we were able to quantify emissions from biomass burning. Using both near-field (< 1 day) and far-field (> 1 day) sampling, boreal forest fire plumes were identified throughout the troposphere. Fresh plumes from fires in Northwest Ontario yield emission factors for CH_4 and CO_2 of 8.5 ± 0.9 g (kg dry matter)$^{-1}$ and 1512 g ± 185 g (kg dry matter)$^{-1}$, respectively. We have also investigated the efficacy of calculating emission factors from far-field sampling, in which there might be expected to be limited mixing with background and other characteristic air masses and we provide guidance on best practice and limitations in

such analysis. We have found that for measurements within plumes that originated from fires in Northwest Ontario 2–4 days upwind, emission factors can be calculated that range between 1618 ± 216 and 1702 ± 173 g (kg dry matter)$^{-1}$ for CO_2 and 1.8 ± 0.2 and 6.1 ± 1 g (kg dry matter)$^{-1}$ for CH_4.

1   Introduction

The global burden of greenhouse gases (GHGs) has increased significantly over the last century. This has mostly been attributed to growth and changes in anthropogenic emissions (Forster and Ramaswamy, 2007). However, trends in globally averaged concentrations alone are not sufficient to predict future changes in the abundance of GHGs and plan mitigation strategies for emission controls. Therefore, the distribution of GHGs needs to be known at a much finer scale, whilst both sources and sinks must be resolved in terms of their process, temporal and spatial variability (Marquis and Tans, 2008; Dlugokencky et al., 2011).

Biomass Burning (BB) has long been known to play an important role in the budgets of a variety of atmospheric trace gases and particles, including GHGs (Crutzen et al., 1979; Seiler and Crutzen, 1980). It is estimated that between 1997 and 2009, global BB released on average 2.0 Pg yr^{-1} of carbon (C) into the atmosphere (van der Werf et al., 2010). However, there is a large degree of uncertainty and variability in the contributions made by particular regions, both intra- and inter-annually. This is due to the unique and episodic nature of individual fire events and the necessary assumptions inherent in the calculation of such emissions coupled with incomplete monitoring. Broadly, however, it has been suggested (van der Werf et al., 2010), that Africa makes the largest contribution to total C emissions (54 %), followed by South America (15 %). Fires in boreal regions have also been attributed to large observed changes in atmospheric composition. For example, forest fires in Russia alone have been causally linked to the accelerated growth rate of global mean CH_4 concentrations that was ob-

Full Screen / Esc

served in 1998, 2002 and 2003 (Dlugokencky et al., 2001; Langenfelds et al., 2002; Simpson et al., 2006).

Climate change has the potential to further increase the impact of wildfires on trace gas budgets. Canadian boreal fire frequency and annual burn area have shown an
5 upward trend since satellites were first able to monitor fires in the 1970s, which is thought to be due to rising mean summer temperatures in the region observed over the same period (Gillett et al., 2004). Current research suggests that this trend will continue: estimates using global circulation models suggest that fires in Canada will be 30 % more frequent by 2030 and could be up to 150 % more common by the end of the
10 century (Wotton et al., 2010).

As well as being a major source of greenhouse gases, BB can significantly reduce air quality on local to hemispheric scales, with emission advected by synoptic weather systems (Damoah et al., 2004). On occasion these long range transported pollutants can lead to exceedances of air quality standards many 1000s km from the fire source
15 (Jaffe et al., 2004). BB influence can also dominate the abundance of various volatile organic compounds (VOCs) measured at remote background sites (Lewis et al., 2013). Under certain burning and meteorological conditions, vertical mixing can be dramatically enhanced by fires (known as pyroconvection), allowing rapid transport of pyrogenic species and particulates into the upper troposphere/lower stratosphere (UTLS),
20 resulting in perturbations to the Earth's radiation budget, cloud microphysics and stratospheric chemistry (Damoah et al., 2006; Cammas et al., 2009). However, much work is still needed to fully understand the relative impact of BB on overall atmospheric composition (Wotawa and Trainer, 2000; Monks et al., 2009); a particular area of disagreement in the literature is whether BB results in the net production of tropospheric
25 O_3 (Jaffe and Wigder, 2012; Parrington et al., 2013).

The BORTAS (Quantifying the impact of BOReal forest fires on Tropospheric oxidants over the Atlantic using Aircraft and Satellites) project was conceived to investigate the distribution and composition of the outflow from North American BB using a combination of ground based, aircraft and satellite measurements, and to use chem-

istry transport models to quantify its impact on tropospheric chemistry. The UK's Facility for Airborne Atmospheric Measurements (FAAM) BAe-146 research aircraft was deployed to Nova Scotia, Canada where a number of BB plumes of differing ages were sampled (0 to 10 days). A comprehensive description of the motivation for the BORTAS experiment can be found in Palmer et al. (2013), along with a description of the FAAM BAe-146 instrumental payload, a general summary of the flights that took place during BORTAS, and the prevailing synoptic meteorological conditions.

This paper presents the in situ observations of CO_2 and CH_4 that were made using cavity enhanced absorption spectroscopy on the FAAM BAe-146 as part of the BORTAS project. In Sect. 2, we describe measurement techniques and analysis methodologies. Section 3 presents bulk statistics using all available measurements, BORTAS measurements are shown to be in agreement with both previous measurements and modelled concentrations. In this section we also identify individual biomass burning events where enhancement ratios and emission factors can be quantified. The paper is briefly summarised in Sect. 4.

2 Data sources and analysis methodology

2.1 Aircraft sampling

The airborne measurement component of BORTAS consisted of 15 flights by the FAAM BAe-146, conducted between 12 July and 3 August 2011. The whole flight campaign comprised approximately 79 h in total, with each flight lasting between 3 and 8 h in duration. These flights are nominally referenced as B618 to B632 and their geographic coverage is shown in Fig. 1. For the majority of the campaign the aircraft was based out of Halifax, Nova Scotia (Palmer et al., 2013).

CO_2 and CH_4 dry air mole fractions were determined using an adapted system based on a Fast Greenhouse Gas Analyser (FGGA) from Los Gatos Research Inc, which uses the cavity enhanced absorption spectroscopy technique. O'Shea et al. (2013) provides

an extensive description of this system along with the associated data processing and quality control procedures that were performed. In-flight calibrations were frequently performed using three gas standards, all of which are traceable to the WMO (World Meteorological Organisation) recommended scales for CO_2 and CH_4 measurements.

5 Through summing all known uncertainties the accuracy of the measurements can be estimated to be ±1.28 ppb for CH_4 and ±0.17 ppm for CO_2. This represents less than 0.1 % and 0.05 % of typical background concentrations, respectively. The 1 Hz precision is 2.48 ppb (1σ) for CH_4 and 0.66 ppm (1σ) for CO_2.

We shall also use concentration data for a range of other trace gases (including those

10 principally emitted by BB) for airmass history as described in Sect. 2.2. This includes carbon monoxide (CO), a product and tracer of incomplete combustion processes; and hydrogen cyanide (HCN) and acetonitrile (CH_3CN), both key tracers of BB. CO was measured using a vacuum ultraviolet florescence analyser, (AL5002, Aerolaser GmbH, Germany; Gerbig et al., 1999). Precision of the 1 Hz CO measurements is ±1.5 ppb at

15 100 ppb; total uncertainty is estimated to be ±2 %.

HCN was monitored using chemical ionisation mass spectrometry (CIMS), with a limit of detection of 5 ppt and a total uncertainty estimated to be 10 % at 3 s time resolution (Le Breton et al., 2013). CH_3CN concentrations were determined using a proton transfer reaction mass spectrometer (PTR-MS), with a 9 to 20 s time response de-

20 pending on the number of species that are measured, and the CH_3CN measurement uncertainty is estimated to be ±9 % (Murphy et al., 2010). For a description of all other measurements made on the FAAM BAe-146 refer to Palmer et al. (2013).

2.2 Analysis methodology

In Sect. 3, we will discuss measurements of various trace gases in the context of their

25 air mass history. To distinguish between air masses we make use of a variety of coincident tracer measurements made on board the FAAM BAe-146. As well as being a tracer for incomplete combustion CO is also produced from the oxidation of hydrocarbons. Reaction with the hydroxyl radical (OH) is the major atmospheric sink.

HCN and CH$_3$CN are principally emitted to the atmosphere by BB (70–85 % for HCN and 90–95 % for CH$_3$CN, Li et al., 2003), and in contrast to CO have minimal anthropogenic sources. Ocean uptake and oxidation by OH are the primary and secondary loss mechanisms for both species (de Gouw et al., 2003; Li et al., 2003). CO, HCN and

5 CH$_3$CN all have atmospheric lifetimes of over a month (de Gouw et al., 2003; Li et al., 2003). It can therefore be assumed that these species are inert dispersive tracers for plumes intercepted when they are less than approximately a week old, since chemical losses over this period should be small. These lifetimes are also short enough so that BB emissions are a substantial increase over the ambient concentrations. For

10 these reason all three species are widely used tracers for BB (Hecobian et al., 2011; Hornbrook et al., 2011; Vay et al., 2011).

To allow comparison between species that were measured using different instruments with different response times a number of different data merges were used. When describing the bulk distribution encountered (Sect. 3.1) 10 s averaged measure-

15 ments were employed, but when examining the individual BB case studies higher resolution measurements of 3 s, were applied.

To probe the history of the air masses encountered by the FAAM BAe-146 we used single-particle 3-dimensional (vertical motion enabled) back trajectories from the offline Hybrid Single-Particle Lagrangian Integrated Trajectory (HYSPLIT) model (Draxler and

20 Rolph, 2003) with National Centre for Environmental Prediction (NCEP) reanalysis meteorological fields at 2.5° spatial resolution on 17 levels. Five-day back trajectories (with half-hourly outputs) were calculated with endpoints co-located with the aircraft position as reported by GPS at 60 s intervals along the aircraft flight track. This method allows us to qualitatively describe air mass history and advection representative of the aircraft

25 sampling, and mimics ensemble analysis in a more tailored way using aircraft flight tracks as the variable parameter rather than perturbations to the reanalysis dataset. It should be noted that this method does not represent a source-inversion and is used here to guide our analysis in terms of qualitative airmass history and general source regions.

The UK Met Office Numerical Atmospheric-dispersion Modelling Environment (NAME) (Jones et al., 2007) was used to complement the back trajectories generated using HYSPLIT. NAME is a stochastic Lagrangian particle dispersion model that can be run both forwards and backwards in time. NAME can use single site observations or 3-D meteorological data to drive the dispersion of the model particles. In this work we have used numerical weather prediction data from the UK Met Office Unified Model (Davies et al., 2005). These are operational analysis fields with a spatial resolution of 0.35° longitude by 0.23° latitude with 59 vertical levels (model top at $\sim$ 30 km). NAME has previously been used to examine the dispersal of particulate matter originating from Russian agricultural fires and its impact on UK air quality (Witham and Manning, 2007). In this work we performed two sets of NAME simulations. The first simulations (not discussed further) were performed in order to simulate the dispersal of the biomass burning plumes that may have influenced our measurements. We focus here on the second set of simulations. These involved releasing 100 000 particles/trajectories over a 1 min period from the locations (latitude, longitude, altitude, time) of a selected number of aircraft observations. The locations of the particles were tracked over a 5 day period going backwards in time. Our analysis focuses on the total column and surface (0 to 200 m a.g.l.) time integrated latitude-longitude distribution of particles.

3   Results and discussion

3.1   Large scale distribution

For the purpose of providing a useful dataset for wider climatological statistics, we present a broad summary of the BORTAS project using all sampled data, excluding the Atlantic transits to Halifax, to represent composition statistics consistent with boreal biomass burning that may be linked to satellite fire observations. Observations on board the FAAM BAe-146 during the BORTAS flights are summarised in Fig. 2 and

overall campaign statistics are shown in Table 1. Notable features of the CO_2 altitude profile are the consistently depleted near surface concentrations, likely due to uptake by the biosphere. This hypothesis is supported by the enhancements in biogenic VOCs that generally occurred during periods of CO_2 depletion. For example, at low altitudes (< 1000 m) the mean concentration of isoprene (C_5H_8), which is principally emitted to the atmosphere from terrestrial plants (Guenther et al., 2006), is a factor 6 larger for the lower CO_2 quartile than it is for the higher CO_2 quartile. In contrast to CO_2, the near surface CH_4 levels are in general enhanced by several tens of ppb compared to those aloft, suggesting significant localised and land-based sources in the region.

On Sable Island, approximately 100 km south east of Halifax a WMO regional monitoring station makes long-term GHG observations. Given the different sampling domain, the BORTAS campaign statistics are in good agreement with the GHG measurements made on Sable Island (WDCGG, 2013). The mean CO_2 concentration on Sable island during the BORTAS sampling period was 386.5 ppm, 1.7 ppm higher than the BORTAS campaign mean (Sable Island CO_2 statistics: median = 385.7 ppm and inter-quartile range 384.2 to 388.5 ppm). The mean CH_4 concentration on Sable Island of 1864 ppb is 5 ppb higher than the FAAM BAe-146 measurements (Sable Island CH_4 statistics: median = 1860 ppb and inter-quartile range 1856 to 1872 ppm).

Two previous airborne measurement campaigns have been performed within both a similar sampling domain and time of year as BORTAS. These are the 2008 ARCTAS experiment (Arctic Research of the Composition of the Troposphere from Aircraft and Satellites, described by Jacob et al., 2010) and the 1992 ABLE-3B experiment (Arctic Boundary Layer Expedition, Harriss et al., 1994). The airborne sampling portion of ARCTAS consisted of both spring and summer campaigns over much of the North American sub-Artic. During the summer deployment CO_2 measurements had a mean of 382.8±3.0 ppm and median 383.1 ppm, marginally lower than those during BORTAS. However, the ARCTAS project experienced a wider range of concentrations, 368.3 to 624.2 ppm. These very high concentrations were due to sampling intense boreal fires in the near-field. Whilst median free tropospheric CO_2 values for each altitude bin range

shown in Fig. 2 compare within several ppm to those observed during the ARCTAS summer deployment (Vay et al., 2011), BORTAS CH_4 concentrations were also found to be generally similar to those during ARCTAS (Singh et al., 2010), as were other species such as CO and O_3 (Parrington et al., 2013). Similar vertical CH_4 gradients to those shown in Fig. 2 were observed during ABLE-3B. However, the baseline ABLE-3B CH_4 concentrations are approximately 100 ppb lower (Wofsy et al., 1994), reflecting the growth of global CH_4 concentrations during the intervening 20 yr period between the two projects (Dlugokencky et al., 2011).

Pollution events are evident in Fig. 2c–d since CO and CH_3CN have many high concentration outliers of an episodic or transitory nature that are many times larger than the cleaner conditions exhibited in the lower quartile. These extreme concentrations, largely associated with BB, are distributed across all altitudes showing that BB not only impacts the region surrounding the fire but it is capable of causing changes in composition throughout the troposphere.

A common method to identify BB plumes is to use some combination of HCN, CH_3CN and CO to partition air masses between those that have, and those that have not, been recently influenced by biomass burning (Hornbrook et al., 2011; Vay et al., 2011; Palmer et al., 2013). A representative threshold concentration value and/or ratio is chosen from tracer-tracer relationships, where the tracer measurements above a certain threshold value are classified as a biomass burning plume. There are a variety of methods that can be used to choose the threshold, but no consistent method is used within the literature (Le Breton et al., 2013), as the chemical background to each dataset or region may be different, requiring unique and tailored analysis. The choice of threshold must also take account of plume age, as typical plumes will continuously mix (dilute) with background air until they become indistinguishable from each other. For long-lived species, such as CO_2 and CH_4, BB will always make some contribution to their global mean background, further necessitating a tailored approach appropriate to the dataset under analysis.

Clear evidence for enhancements due to BB can be found in the BORTAS CO_2 and CH_4 datasets. This is shown in Fig. 3, where the scatter plots have been colour coded by CH_3CN as a tracer for BB. However, these enhancements are proportionately quite small compared to their background levels and are obscured by variability in CO_2 and CH_4 that is not associated with changes in CH_3CN, suggesting that additional (possibly anthropogenic as well as biogenic) fluxes are influencing concentrations. As a consequence the correlation with CO across all flights is weak ($R^2 = 0.09$ for CO_2 and $R^2 = 0.12$ for CH_4). This is in contrast to the majority of VOCs, where the typical enhancements are several times larger than their background and the influence of BB on the dataset is much more distinct (Lewis et al., 2013).

The flights during the BORTAS experiment had the explicit aim of intercepting BB, and therefore the measurements discussed here do not represent a random sample of the atmosphere during this measurement period, but rather a targeted sampling of air masses that have been influenced by BB. To analyse the background measurements we filter the dataset for measurements made when the HCN and CH_3CN concentrations are below the median for the campaign, 76 ppt and 137 ppt, respectively. This will remove the influence of BB from all but the smallest and most well mixed plumes to give a confident background concentration. Using this criteria, the correlation between CH_4 and CO_2 is much stronger ($R^2 = 0.72$) giving us good confidence in our choice for the BORTAS dataset. A negative relationship is found with regression slope (-5.31 ± 0.01) $\times 10^{-3}$ mol CH_4 (mol CO_2)$^{-1}$. A negative correlation is consistent with a combination of CO_2 uptake by the biosphere within the region and surface emissions of CH_4. Biogenic CH_4 to CO_2 flux ratios have shown a wide degree of variability, for example ground based eddy covariance flux measurements found the flux ratio to vary between -56 and -2×10^{-3} mol CH_4 (mol CO_2)$^{-1}$ from Californian rice fields over the growing season (McMillan et al., 2007).

Ethane (C_2H_6) shares several common sources with CH_4: BB, combustion of fossil fuels and biofuels; however it does not have a biogenic source. For this reason simultaneous measurement of C_2H_6 can aid the apportionment of CH_4 sources (Simpson

et al., 2012). Correlation between C_2H_6 and CO is much stronger than it is for CH_4 (R^2 = 0.95 for all measurements, Lewis et al., 2013) whilst for both plume and non-plume measurements correlation between C_2H_6 and CH_4 integrated across all flights during BORTAS is poor (R^2 < 0.3). However, correlations for background measure-

5 ments on individual flights was noted to range widely with a peak of 0.95 in flight B624 (for 8 samples) and a minimum of 0.05 in flight B622 (for 5 samples). This would suggest that the variability in non-fire (background) CH_4 concentrations is generally due to biogenic emissions. However, it should be noted that the C_2H_6 observations were retrieved by analysing 529 flask samples collected at specific but irregular points in time

10 and therefore we do not have equivalent spatial or temporal resolution with the continuous in-situ CH_4 and CO measurements, nor the quantity of samples, from which to fully investigate the relationship to C_2H_6 in the same way that we are able to for the 0.1 Hz in situ measurements.

Examining bulk statistics for all science flight measurements, CO_2 and CH_4 con-

15 centrations made in BB plumes are only marginally different to those outside of plumes (Table 1). For CO_2 the mean in plume concentration is only 2 ppm higher than the mean out of plume and within analytical uncertainty the mean CH_4 concentrations are identical. In Sect. 3.2 we identify individual case studies in the dataset where enhancements due to BB can be quantified.

20 As reported by Palmer et al. (2013) fire activity during the BORTAS sampling period was dominated by widespread fires in Northwest Ontario. Extensive fires in this region took place from 17 to 19 July 2011, plumes from which were sampled over 1000 km downwind during measurement flights B621 to B624 (18 to 21 July 2011, Sect. 3.2.2). This region was also sampled in the near-field on 26 July 2011 (B626,

25 Sect. 3.2.1), however, at this time, fire activity in the region was reduced and the plumes more localised. The flights later in the campaign (B628, 28 July 2011) sampled plumes that were reported to be over 7 days old (Parrington et al., 2013). Concentrations in these plumes were relatively low with CO reaching 135 ppb, HCN 330 ppt and CH_3CN

310 ppt, nevertheless the correlation between HCN and CO (R^2 = 0.69 for the whole flight) implies that they are still representative of a biomass burning origin.

As a tracer for incomplete combustion, CO enhancements are characteristic of not only BB but also anthropogenic activity. Throughout the BORTAS dataset regions of enhanced CO are almost entirely coincident with enhancements in CH_3CN (R^2 = 0.89 for all measurements, Fig. 3) suggesting that anthropogenic emissions are well mixed and local sources had a minimal influence on the BORTAS dataset. An exception to this occurred during flight B629, which briefly overflew the Dartmouth Oil refinery located on Halifax Harbour, NS. Whilst overflying the refinery, CO_2 was enhanced by 8 ppm over the local average background and enhancements were also noted in NO_x (NO up to 3.3 ppb and NO_2 up to 3.8 ppb). The high partitioning of NO/NO_2 suggests that this is a photo-chemically fresh plume and therefore local in origin. We note that there was no observable significant change in CO and CH_4 or BB tracers (e.g. CH_3CN).

3.2 Comparison to MACC model composition

To discuss trace gas measurements as recorded during BORTAS in the context of sources of composition model bias, we compared the in situ measurements of CO_2, CH_4 and CO on the FAAM BAe-146 to those from the Monitoring Atmospheric Composition and Change (MACC) project (Inness et al., 2013). The global MACC reanalysis service provides a reanalysis for the years 2003 to 2012 of trace gas and aerosol concentrations, with the reactive gases reanalysis system produced by the coupled Integrated Forecasting System-Model for ozone and related chemical tracers (IFS-MOZART) modelling and assimilation system. Benedictow et al. (2013) gives the latest validation report on the MACC reanalysis product.

This comparison is shown in Fig. 4. The MACC fields used are statistics that have been determined over the corresponding BORTAS measurement period of 18 July to 21 July 2011 for the whole sample region covered by the FAAM BAe-146, excluding the Atlantic transits to and from Cranfield, UK, (a geographic region of 40 to 60° N and

40 to 100° W). Since the MACC fields have not been sampled at the exact time and position of the FAAM BAe-146 flights, precise agreement between measurement and model is not expected. However, the comparison is instructive since it tests the model's skill at simulating the large-scale features and typical background concentrations in the region.

For CO, the MACC is able to reproduce both the high concentrations from episodic BB events (through emission inventories augmented with MODIS fire information, as well as CO observations from IASI and MOPITT were assimilated during the reanalysis experiment) and the approximate background levels with reasonable agreement to the measurements. The mean difference between the medians for individual altitude bins is ∼ 5 ppb (comparable to the total column bias) and the inter-quartile ranges generally agree. The large negative CO biases observed by Inness et al. (2013) are not seen here, possibly because that comparison found the largest discrepancies in the boundary layer at urban sites affected by pollution.

Similarly good agreement is seen for CO_2 where the median concentrations for each altitude bin are typically within 1 ppm and the inter-quartile ranges are comparable. The very low CO_2 concentrations within the lowest altitude bin are a known spurious result present in the MACC data set.

MACC is also able to simulate the general structure of the CH_4 altitude profile. However there exists a significant disagreement over the absolute concentrations, MACC typically under estimates CH_4 by approximately 75 ppb. This deviation is sufficiently large and consistent in the vertical, that it is unlikely to be a result of the BORTAS sampling strategy. Detailed analysis of this disparity is beyond the scope of this paper but we note it here as a source of potential model bias.

3.3 Enhancement ratios and emission factors

The enhancement in a species' concentration is not usually used to assess BB impact on trace gas budgets, since it is largely dependent on how diluted a plume has become as it mixes with background air (LeCanut et al., 1996). Instead, trace gas emis-

sions from biomass burning are often expressed as either an emission ratio (ER) or an emission factor (EF). An ER for a species, X, is the number of molecules of this species emitted into the atmosphere per molecule of a tracer for biomass burning, usually CO_2 or CO. It is equal to the regression slope of the measurements of X in a plume versus the simultaneous measurement of the tracer species. To calculate ERs we use an orthogonal distance regression, weighted by the measurement uncertainty. The uncertainties given are the standard deviation of the fit. Correlation coefficients (R^2) have also been included, which have been calculated using least squares regression. ERs can also be calculated by first subtracting the background concentrations from the in the plume measurements. However we have chosen not to use this approach, due to the subjective nature of choosing a background. As a BB plume moves away from its source, chemical reactions may enhance or deplete a particular species and as a consequence the determined ER. For this reason, the ER for short-lived species should only be calculated using measurements in the freshest possible fire plumes. In aged plumes the term normalised excess mixing ratio (NEMR) is usually used instead (Akagi et al., 2011).

While an EF is the mass of the species emitted for every kg of dry biomass burnt, it is usually calculated using the carbon mass balance technique (Andreae and Merlet, 2001; Christian et al., 2007; Simpson et al., 2011; Akagi et al., 2012). This is based on the assumption that all combusted carbon (C) is measured in the plume. The EF, in g of X per kg of dry matter burnt, can be calculated using Eq. (1):

$$EF = F_c \cdot \frac{M_X \Delta C_X}{M_c \Delta C_T} \qquad (1)$$

where F_C is the fraction of C in the fuel. This is chosen to be $500\,\mathrm{g\,kg^{-1}}$ and is thought to be accurate to $\pm 10\%$ (2σ) (Susott et al., 1996; Yokelson et al., 1999). M_X and M_C are the molecular masses of species X and carbon ($12.011\,\mathrm{g\,mol^{-1}}$), respectively. $\Delta C_X / \Delta C_T$ is the ratio of the number of moles of species X to the total number of moles of carbon emitted by the fire. This can be calculated using the ER, when CO is used as

a tracer, of X ($\Delta[C_X]/\Delta[CO]$) and all the other C containing molecules in the plume. It is not possible to measure all C containing molecules, so we approximate total C using only CO_2, CO and CH_4. This will result in an overestimate of the true value, but this is only expected to amount to a few percent. Simpson et al. (2011) measured CO_2, CO, CH_4 and 80 non-methane VOCs in Canadian biomass burning plumes and found that 98.6 % of the measured C was either in the form of CO_2, CO or CH_4. We can then calculate $\Delta C_X/ \Delta C_T$ using Eq. (2):

$$\frac{\Delta C_X}{\Delta C_T} = \frac{\frac{\Delta[C_X]}{\Delta[CO]}}{1 + \frac{\Delta[CO_2]}{\Delta[CO]} + \frac{\Delta[CH_4]}{\Delta[CO]}} \tag{2}$$

3.3.1   Near field biomass burning: 26 July 2011 plume

The flights during the BORTAS project had the aim of sampling BB plumes that were a variety of ages. Only Flight B626 (26 July 2011) sampled fresh plumes. This flight consisted of a transit from Halifax, Nova Scotia, followed by a boundary layer survey over an active fire region in Northwest Ontario ($\sim$ 52.5° N, $\sim$ 93.6° W), before landing at Thunder Bay, Ontario. We concentrate our analysis here on the low-level portion of the flight (900 m to 1100 m). Figure 5a shows a time-series of BB tracer concentrations whilst repeatedly penetrating a number of plumes, where the BB tracers discussed in Sect. 2 were clearly elevated above their local background.

At such close proximity to the fires the plumes are of limited spatial extent (of the order 1 km), it is therefore beneficial to use higher frequency measurements (0.33 Hz) for analysis rather than the 0.1 Hz measurements that have been used previously. Unfortunately, CH_3CN measurements are not available at this high frequency. We therefore use the method described by LeBreton et al. (2013), using HCN and CO, to determine whether BB has recently influenced an air mass. Firstly, the HCN and CO time series are examined for periods out-of-plume during the low-level flying that represent a typical background. For CO and HCN this was facilitated by relatively large enhance-

ments (up to factor 15) in the plume. The mean and standard deviation of the background regions were then determined. Measurements made when the simultaneous CO and HCN mole fraction were 6 standard deviations greater than their background were deemed to be in a BB plume. It should be noted that the measurements are not normally distributed (due to non-random sampling) and as a result no assumption should be made about the proportion of measurements within 1 standard deviation of the mean. The 6 standard deviation threshold is only used to represent a significant enhancement over the background.

For CO the background has a mean of 105 ppb with a standard deviation of 9 ppb, while HCN had a mean of 259 ppt with standard deviation of 50 ppt. These CO concentrations are typical of the background levels encountered during both this project (Fig. 2) and previous measurements made in similar locations (Vay et al., 2011). A lack of field measurements mean that the distribution of HCN in the troposphere is not as well known as it is for CO. Mean tropospheric HCN concentrations from previous studies were found to be 243 ± 118 ppt (Singh et al., 2003) and 220 ppt (Li et al., 2003), comparable to the background that we determine. Tracer-tracer scatter analysis of CO_2, CH_4 and CO measurements are shown in Fig. 5b–c. For both CO_2 and CH_4, strongly correlated ($R^2 = 0.95$ for CH_4 and $R^2 = 0.69$ for CO_2) linear relationships were found for the BB plume measurements as expected. Since the flight traversed across a small region several times we group the observed enhancements together to calculate ER's of 0.079 ± 0.001 mol CH_4 (mol CO)$^{-1}$ and 5.9 ± 0.4 mol CO_2(mol CO)$^{-1}$. From these ER's, using Eq. (1) and Eq. (2), EFs of 8.5 ± 0.9 g (kg dry matter)$^{-1}$ and 1512 ± 185 g (kg dry matter)$^{-1}$ can be calculated for CH_4 and CO_2, respectively. Calculated EFs are in good agreement with previous studies in boreal regions (see Table 2), as are those for CO and HCN (not shown).

To examine the sensitivity of the choice of threshold on the determined EF, we repeated the analysis varying the threshold from 0 to 20 standard deviations above the background. For both CH_4 and CO_2 the correlation with CO increases as the threshold rises, as would be expected from removing non-BB sources from the dataset used in

the EF calculation. The increase in correlation is more dramatic for CO_2 than CH_4 (for all thresholds the CH_4 versus CO R^2 is always greater than 0.8). Apart from standard deviation thresholds less than 6, the determined EFs are within 10 % of each other, lending confidence in our choice of this threshold whilst simultaneously providing po-
tential uncertainty that this compromise may impose. This highlights the importance of examining the sensitivity of the determined ER and EF to the method used to define a BB plume. A higher sensitivity is expected to be found when relatively few data points exist in a plume compared to those in background regions, as was the case for B626. We acknowledge this extra uncertainty and use a 6 standard deviation approach for
calculating NEMR and EFs in aged plumes.

An emission rate for a species can be estimated by combining its EF with an estimate of the total matter burnt e.g. using The Global Fire Emissions Database (van der Werf et al., 2010). However, a single EF is not sufficient to describe emissions within a particular biome or even an individual fire that will go through several distinct combustion
phases with different EFs. A review of the variables that influence the EF is provided by van Leeuwen and van der Werf (2011). These include factors related to the material burnt (size, density, water content, vegetation spacing) as well as meteorological factors (wind speed, humidity, precipitation, temperature). For this reason we include the modified combustion efficiency (MCE, Eq. 3) in Table 2 as a measure of whether a fire
is predominantly in the flaming or smouldering phase.

$$MCE = \frac{1}{1 - \frac{\Delta[CO]}{\Delta[CO_2]}} \tag{3}$$

Laboratory studies suggest that this varies from 0.8 for purely smouldering combustion to 0.99 for purely flaming combustion (Yokelson et al., 1996).

An MCE of 0.83 ± 0.01 is characteristic of smouldering combustion, which would
typically result in proportionally more reduced compounds being released. This will likely be the reason for a relatively large amount of CH_4 being released compared to previous studies. van Leeuwen and van der Werf (2011) grouped CH_4 EFs in the

Campaign climatology, airmass analysis and enhancement ratios

S. J. O'Shea et al.

Title Page

Abstract	Introduction
Conclusions	References
Tables	Figures

◄ | ►

◄ | ►

Back | Close

Full Screen / Esc

Printer-friendly Version

Interactive Discussion

literature based on biome and the fires MCE. The EF calculated for B626 shows an excellent agreement with the amount of CH_4 emitted for a fire with its combustion efficiency as predicted from their work.

3.3.2 Far-field biomass burning: 18 to 21 July 2011 plumes

5 In theory, as long as the atmospheric lifetime of a species is significantly longer than the age of a plume, it should be possible to calculate ER using measurements in plumes that are several days old, since the calculated NEMR should be approximately equal to the ER at source. However, due to the strong vertical gradients in CO_2 and CH_4 (Fig. 2) that were observed over Canada, further consideration needs to made before NEMRs
10 can be calculated for plumes that have been lofted out of the boundary layer into the free troposphere. When a plume is sampled at several altitudes it can be expected that it may have mixed with background air with composition reflecting different origins. As a result when the profile is examined as a whole, strong correlation between two pyrogenic species may not be observed and the uncertainty in the calculation of a NEMR
15 would be large. This lack of correlation may also be due to several different ERs at source that mix during transport to the receptor site.

From 18 to 21 July 2011 four measurement flights took place (B621 to B624), during which a number of air masses were intercepted that had clearly been influenced by BB. HYSPLIT back trajectories suggest that these plumes originated 2 to 4 days previously,
20 from fires in western Ontario (Fig. 6). Figure 7b, c shows how the trajectories were used to identify the source of the fire, Fig. 7b shows 5 day back trajectories with endpoints co-located with the FAAM BAe-146 for the entire flight. When the trajectories are selected that are associated with the enhanced CO and HCN (Fig. 7c) the majority overpass a region in Northwest Ontario that is identified as having had active fires as observed by
25 MODIS. We acknowledge that HYSPLIT trajectories are not able to simulate the added buoyancy of a fire plume (pyroconvection), therefore the plume injection profile near to the fires is not known, and as a consequence these air masses may have potentially been influenced from further afield such as Northern Alberta and the North Western

Territories, for B621 and B623 in particular (Fig. 6). However, Parrington et al. (2013) determined a similar age for these plumes by comparing ratios of VOCs to estimate the degree of photochemical processing that the plumes had experienced and hence an approximate age.

5   To investigate this further, we also examined dispersion model ensembles and surface footprints. NAME column integrated dispersion plots (Fig. 8) show sampled airmasses that were associated with BB passed over the same fire region in northwest Ontario as indicated in the HYSPLIT trajectories (Figs. 6 and 7). Column integrated particle dispersion fields from NAME for flight B622 and B623 are shown in Fig. 8.

10 However when examining only the surface footprint over the 5 day airmass history (see the bottom panels of Fig. 8), we see a mixed picture. For B622 (Fig. 8d), there is a footprint in proximity to the fires detected by MODIS. However, for B623 (Fig. 8b), there is little evident surface contact over the 5 day history in regions with significant fire activity. This nicely illustrates the efficacy and pitfalls of airmass history analysis

15 using Lagrangian trajectory and dispersion models run backwards in time. For B622, NAME guides us well in the surface attribution of BB sources, while for B623, if we were not otherwise expectant of dynamics such as active pyroconvection (Gonzi and Palmer, 2010; Glatthor et al., 2013), then NAME would point to more distant surface sources. The fact that all trajectories (both HYSPLIT and NAME) pass over the fire

20 region is consistent with the injection of material into those higher level trajectories by pyroconvection, which is known to be active in the area.   Without prior knowledge of the injection profile of material it is not possible to accurately model dispersion in the forward frame, yet these dynamical history fields from NAME and HYSPLIT together nicely illustrate the passage of air over the fire region.

25 Whilst aircraft in situ measurements are essential for giving highly accurate quantitative information about the background and plume concentrations, their limited spatial coverage means that it is often difficult to map the full extent and movement of the plume purely from these measurements. Satellite measurements, whilst limited in their sampling and vertical sensitivity, are able to inform on these large spatial scales. The In-

Title Page

Abstract	Introduction
Conclusions	References
Tables	Figures

|◄ | ►|

◄ | ►

Back | Close

Full Screen / Esc

Printer-friendly Version

Interactive Discussion

frared Atmospheric Sounding Interferometer (IASI) is a nadir viewing instrument flying operationally on the MetOp-A satellite. IASI Total Column (TC) CO (daytime overpass) values, retrieved using the FORLI algorithm (Kerzenmacher et al., 2012) are visually compared here to the FAAM BAe-146 CO in situ concentrations (Fig. 9), to provide further illustration that the enhanced concentrations of CO came from in-plume sampling. As well as showing enhancements in approximately the same location as those identified by the FAAM BAe-146, IASI shows the plume to cover much of the Eastern Canadian coast. The satellite measurements also support the suggestion that the plumes originated from fires in Northwest Ontario.

Flight B621 (18 July 2011) travelled east from Halifax, NS refuelling in Goose Bay, NL before returning to Halifax, NS. On the outbound transit a significant plume was intercepted to the East of the Gulf of St. Lawrence, between 4 km and 7 km. CH_4 was raised by approximately 100 ppb over the background and concentrations exceeded 1900 ppb, while HCN reached 4.5 ppb. Once the FAAM BAe-146 had descended through the BB plume a trend of increasing CH_4 and decreasing CO_2 could be identified. CO and HCN remain relatively constant during this descent until another layer of BB is encountered at 2 km.

Flights B622 and B623 both took place on the 20 July 2011, B622 travelled from Halifax to Quebec City, while B623 is the return journey. Deep profiles and constant altitude runs were performed over Southern Quebec and New Brunswick. Both CO and HCN showed a high degree of variability and were both elevated throughout much of the flights, over the altitude range 2000 to 8000 m. Peak plume concentrations exceeded 1 ppm and 1 ppb for CO and HCN, respectively.

When the individual flights were analysed as a whole correlations between CO, CH_4 and CO_2 were in general weak ($R^2 < 0.4$). This was still the case when filters for BB were applied using HCN or CH_3CN. For this reason, it is necessary to partition the flights into individual constant altitude runs or profiles to calculate NEMRs. In general, correlation was found to be more robust when the individual runs are examined separately. Table 1 shows NEMRs for all runs and profiles when the correlation coefficient

(R^2) is greater than 0.60. Where possible EFs are also calculated assuming no chemical loss during transport.

The calculated CH_4 EFs range between 1.8 ± 0.2 and $6.1 \pm 1 \, g \, (kg \, dry \, matter)^{-1}$, all of which are lower than the $8.5 \, g \, (kg \, dry \, matter)^{-1}$ that was determined when the Northwest Ontario fires were sampled in the near field. However, the aged plumes have a higher MCE, which is representative of a larger proportion of flaming combustion and therefore a lower proportion of reduced compounds, such as CH_4. This highlights the difficulty in calculating budgets for BB, since fires in one region with approximately the same vegetation type can have such a range of EFs.

However, uncertainties are larger when calculating ER/EF from measurements in aged plumes, an example of this occurred during flight number B624 (21 July 2012). Near the coast of Newfoundland a large biomass burning plume was sampled between ~ 2 and $3 \, km$ altitude. Straight-and-level runs were repeatedly performed into and out of the plume. Figure 7a shows a measurement time-series of several trace gas concentrations during these runs. CO and HCN both show a clear enhancement consistent with a BB plume and there is excellent correlation between the two tracers ($R^2 = 0.94$, Fig. 10a). The HCN to CO NEMR for this plume was found to be $(3.03 \pm 0.02) \times 10^{-3} \, mol \, HCN \, (mol \, CO)^{-1}$. This NEMR is in reasonable agreement with the ratio when sampling BB in the near field both in this study and in previous studies (Simpson et al., 2011). Similarly strong agreement is seen for hydrocarbons such as C_2H_6 ($R^2 = 0.97$) and C_3H_8 (Propane, $R^2 = 0.88$).

The BB plume is not as clearly defined in the CH_4 and CO_2 time series as it is for the other species associated with biomass burning. This is expected to be partly due to their proportionately higher mean background relative to their typical enhancement and also because there are additional non-BB sources and sinks of these gases relative to CO and HCN (e.g. biospheric uptake and wetland biogenic emission). Even though the correlation between CH_4 and CO is still strong ($R^2 = 0.70$), a single mixing line cannot be identified in the scatter plot with CO (Fig. 9b) when using the threshold criterion used in the near-field analysis earlier. This suggests that there may have been mixing

into the plume by a localised source during trajectory from fire source to sampling location. Back trajectories illustrate this diversity. We see that during the flight a variety of air masses were sampled, including some that had recently descended from the free troposphere ($> 4\,km$) over the Arctic in the polar jetstream. As expected, these air masses are associated with the lowest amounts of CO, typically less than 100 ppb. Other trajectories have originated from the southern US.

The trajectories suggest that since being emitted the plume has travelled over central Canada before being sampled. During this time it is likely that the plume will have mixed with air masses containing enhanced CH_4 from biogenic emissions associated with the Canadian wetlands, e.g. the Hudson Bay Lowlands (HBL). This is well known to be a significant source of CH_4 and is thought to comprise approximately 10 % of the global boreal wetland emissions of CH_4 or about $2.3\,Tg\,yr^{-1}$ (Pickett–Heaps et al., 2010). To investigate this further we define the HBL as the geographic region $50°\,N$–$60°\,N$, $75°\,W$–$96°\,W$. Figure 10b colour codes the scatter plot according to the length of time that the trajectories spent in this region below 2000 m and the markers have also been sized depending on the length of time the trajectories spent within this region below 1000 m. The longer an air mass spends at low altitude within this region the more sensitive it will be to HBL as a source of CH_4. An NEMR of 0.170 ± 0.003 ($R^2 = 0.97$) can be calculated for just those air masses that have passed over HBL below 1000 m. Though not unrealistic, this is larger than typically measured for BB, suggesting that the enhancement may not be purely due to BB. As a general point, we report NEMRs for aged plumes with the important caveat that the impacts (and therefore uncertainty) of mixing cannot be quantified using the available dataset. This is an important consideration for existing and future datasets of this type where far-field NEMRs have been calculated and careful analysis of multiple tracers and airmass history must always accompany any such attempt.

A clear region where CH_4 is anti-correlated with both CO_2 ($R^2 = 0.74$) and CO ($R^2 = 0.55$) can be identified (Fig. 9b), with enhancement ratios of $(-3.79 \pm 0.04) \times 10^{-3}$ mol CH_4 (mol CO_2)$^{-1}$ and -0.284 ± 0.003 mol CH_4 (mol CO)$^{-1}$. This could suggest mix-

Title Page

Abstract	Introduction
Conclusions	References
Tables	Figures

◄◄	►►
◄	►
Back	Close

Full Screen / Esc

Printer-friendly Version

Interactive Discussion

ing or advection of an aged fire plume into a region of an enhanced CH_4 surface flux (e.g. biogenic emission of CH_4 over wetlands as noted in the trajectory analysis for this flight earlier). However, this additional mixing renders this particular air mass (represented by the anti-correlated mixing line in Fig. 10b) invalid for calculation of a subsequent NEMR. We note the existence of this air mass here for purposes of completeness and by way of advice when working with aged plumes that may have been influenced along their trajectory. Careful analysis and selection of data must be performed to remove sources of bias such as this in NEMR calculation of plumes which are otherwise still viable as representative of BB.

4 Conclusions

Airborne in situ measurements of CO_2, CH_4 and other trace gases were made over eastern Canada, using the FAAM BAe-146 research aircraft, as part of the BORTAS experiment. Both CO_2 and CH_4 showed a wide degree of variability, which ranged 371.5 to 397.1 ppm for CO_2, and 1797 to 1968 ppb for CH_4, representing the unique nature of the various fire plumes sampled. Vertical concentration profiles were found to be broadly comparable with previous measurements, such as those from the ARCTAS project and reanalysed composition fields, that assimilate IASI/MOPITT satellite measurements, from the European Union funded MACC project. Source-specific tracers were used to distinguish between air masses. CO_2 extrema were characterised by BB emissions and biospheric uptake, while CH_4 concentrations were dominated by both BB and biogenic emissions. BB plumes were sampled throughout the troposphere over an altitude range of ~ 900 m to ~ 8000 m. Near-field sampling of fires in Northwest Ontario yielded EFs of 1512 ± 185 g (kg dry matter)$^{-1}$ and 8.5 ± 0.9 g (kg dry matter)$^{-1}$ for CO_2 and CH_4, respectively. Using a combination of in-situ HCN measurements, Lagrangian trajectory models and MODIS active fire maps, it was found that plumes from this region were sampled several thousand km downwind when they were 2 to 4 days old. It was found that significant uncertainties exist when calculating EF/ERs

from measurements in aged plumes due to the mixing that can occur with non-fire sources during transport such as biogenic emissions in this case and that special care must be taken when interpreting far-field data of this type in both existing and future BB datasets. In these aged plumes, EFs were found to vary between 1618 ± 216 and $1702 \pm 173\,\mathrm{g}\,(\mathrm{kg\ dry\ matter})^{-1}$ of CO_2 and 1.8 ± 0.2 and $6.1 \pm 1\,\mathrm{g}\,(\mathrm{kg\ dry\ matter})^{-1}$ of CH_4. In summary, the results from this study provide a novel set of fire emission factors and climatological statistics that will inform modelling and process-related studies in the Canadian boreal region.

References

Akagi, S. K., Yokelson, R. J., Wiedinmyer, C., Alvarado, M. J., Reid, J. S., Karl, T., Crounse, J. D., and Wennberg, P. O.: Emission factors for open and domestic biomass burning for use in atmospheric models, Atmos. Chem. Phys., 11, 4039–4072, doi:10.5194/acp-11-4039-2011, 2011.

Akagi, S. K., Craven, J. S., Taylor, J. W., McMeeking, G. R., Yokelson, R. J., Burling, I. R., Urbanski, S. P., Wold, C. E., Seinfeld, J. H., Coe, H., Alvarado, M. J., and Weise, D. R.: Evolution of trace gases and particles emitted by a chaparral fire in California, Atmos. Chem. Phys., 12, 1397–1421, doi:10.5194/acp-12-1397-2012, 2012.

Andreae, M. O. and Merlet, P.: Emission of trace gases and aerosols from biomass burning, Global Biogeochem. Cy., 15, 955–966, doi:10.1029/2000gb001382, 2001.

Benedictow, A., Blechschmidt, A.-M., Bouarar, I., Cuevas, E., Clark, H., Flentje, H., Griesfeller, J., Huijnen, V., Huneeus, N., Jones, L., Kapsomenakis, J., Kinne, S., Lefever, K., Razinger, M., Richter, A., Schulz, M., Thomas, W., Thouret, V., Vrekoussis, M., Wagner, A., and Zerefos, C.: The MACC reanalysis: an 8-year data set of atmospheric composition, MACC-II Deliverable D_83.4, available at: http://www.gmes-atmosphere.eu/documents/maccii/deliverables/val/, 2013.

Cammas, J.-P., Brioude, J., Chaboureau, J.-P., Duron, J., Mari, C., Mascart, P., Nédélec, P., Smit, H., Pätz, H.-W., Volz-Thomas, A., Stohl, A., and Fromm, M.: Injection in the lower stratosphere of biomass fire emissions followed by long-range transport: a MOZAIC case study, Atmos. Chem. Phys., 9, 5829–5846, doi:10.5194/acp-9-5829-2009, 2009.

Christian, T. J., Yokelson, R. J., Carvalho, J. A., Jr., Griffith, D. W. T., Alvarado, E. C., Santos, J. C., Neto, T. G. S., Gurgel Veras, C. A., and Hao, W. M.: The tropical forest and fire emissions experiment: Trace gases emitted by smoldering logs and dung from deforestation and pasture fires in Brazil, J. Geophys. Res.-Atmos., 112, D18308, doi:10.1029/2006jd008147, 2007.

Crutzen, P. J., Heidt, L. E., Krasnec, J. P., Pollock, W. H., and Seiler, W.: Biomass burning as a source of atmospheric gases CO, H_2, N_2O, NO, CH_3CL and COS, Nature, 282, 253–256, doi:10.1038/282253a0, 1979.

Damoah, R., Spichtinger, N., Forster, C., James, P., Mattis, I., Wandinger, U., Beirle, S., Wagner, T., and Stohl, A.: Around the world in 17 days - hemispheric-scale transport of forest fire smoke from Russia in May 2003, Atmos. Chem. Phys., 4, 1311–1321, doi:10.5194/acp-4-1311-2004, 2004.

Damoah, R., Spichtinger, N., Servranckx, R., Fromm, M., Eloranta, E. W., Razenkov, I. A., James, P., Shulski, M., Forster, C., and Stohl, A.: A case study of pyro-convection using transport model and remote sensing data, Atmos. Chem. Phys., 6, 173–185, doi:10.5194/acp-6-173-2006, 2006.

Davies, T., Cullen, M. J. P., Malcolm, A. J., Mawson, M. H., Staniforth, A., White, A. A., and Wood, N.: A new dynamical core for the Met Office's global and regional modeling of the atmosphere, Q. J. Roy. Meteor. Soc., 608, 1759–1782, 2005.

Title Page

Abstract | Introduction

Conclusions | References

Tables | Figures

|◄ | ►|

◄ | ►

Back | Close

Full Screen / Esc

Printer-friendly Version

Interactive Discussion

Discussion Paper | Discussion Paper | Discussion Paper | Discussion Paper

de Gouw, J. A., Warneke, C., Parrish, D. D., Holloway, J. S., Trainer, M., and Fehsenfeld, F. C.: Emission sources and ocean uptake of acetonitrile (CH_3CN) in the atmosphere, J. Geophys. Res.-Atmos., 108, 4329, doi:10.1029/2002jd002897, 2003.

Dlugokencky, E. J., Walter, B. P., Masarie, K. A., Lang, P. M., and Kasischke, E. S.: Measurements of an anomalous global methane increase during 1998, Geophys. Res. Lett., 28, 499–502, doi:10.1029/2000gl012119, 2001.

Dlugokencky, E. J., Nisbet, E. G., Fisher, R., and Lowry, D.: Global atmospheric methane: budget, changes and dangers, Philos. T. Roy. Soc. A, 369, 2058–2072, doi:10.1098/rsta.2010.0341, 2011.

Draxler, R. R. and Rolph, G. D.: HYSPLIT (HYbrid Single-Particle Lagrangian Integrated Trajectory) Model, NOAA Air Resources Laboratory, Silver Spring, MD, USA, 2003.

Forster, P. and Ramaswamy, V.: Changes in Atmospheric Constituents and in Radiative Forcing, Climate Change 2007: the Physical Science Basis, 129–234, Cambridge Univ. Press, Cambridge, UK, 2007.

Gerbig, C., Schmitgen, S., Kley, D., Volz-Thomas, A., Dewey, K., and Haaks, D.: An improved fast-response vacuum-UV resonance fluorescence CO instrument, J. Geophys. Res.-Atmos., 104, 1699–1704, doi:10.1029/1998jd100031, 1999.

Gillett, N. P., Weaver, A. J., Zwiers, F. W., and Flannigan, M. D.: Detecting the effect of climate change on Canadian forest fires, Geophys. Res. Lett., 31, L18211, doi:10.1029/2004gl020876, 2004.

Glatthor, N., Höpfner, M., Semeniuk, K., Lupu, A., Palmer, P. I., McConnell, J. C., Kaminski, J. W., von Clarmann, T., Stiller, G. P., Funke, B., Kellmann, S., Linden, A., and Wiegele, A.: The Australian bushfires of February 2009: MIPAS observations and GEM-AQ model results, Atmos. Chem. Phys., 13, 1637–1658, doi:10.5194/acp-13-1637-2013, 2013.

Gonzi, S. and Palmer, P. I.: Vertical transport of surface fire emissions observed from space, J. Geophys. Res., 115, D02306, doi:10.1029/2009JD012053, 2010.

Guenther, A., Karl, T., Harley, P., Wiedinmyer, C., Palmer, P. I., and Geron, C.: Estimates of global terrestrial isoprene emissions using MEGAN (Model of Emissions of Gases and Aerosols from Nature), Atmos. Chem. Phys., 6, 3181–3210, doi:10.5194/acp-6-3181-2006, 2006.

Harriss, R. C., Wofsy, S. C., Hoell Jr., J. M., Bendura, R. J., Drewry, J. W., McNeal, R. J., Pierce, D., Rabine, V., and Snell, R. L.: The arctic boundary layer expedition (ABLE 3B): July–August 1990, J. Geophys. Res., 99, 1635–1643, 1994.

Title Page

Abstract | Introduction

Conclusions | References

Tables | Figures

|◀ | ▶|

◀ | ▶

Back | Close

Full Screen / Esc

Printer-friendly Version

Interactive Discussion

Hecobian, A., Liu, Z., Hennigan, C. J., Huey, L. G., Jimenez, J. L., Cubison, M. J., Vay, S., Diskin, G. S., Sachse, G. W., Wisthaler, A., Mikoviny, T., Weinheimer, A. J., Liao, J., Knapp, D. J., Wennberg, P. O., Kürten, A., Crounse, J. D., Clair, J. St., Wang, Y., and Weber, R. J.: Comparison of chemical characteristics of 495 biomass burning plumes intercepted by the NASA DC-8 aircraft during the ARCTAS/CARB-2008 field campaign, Atmos. Chem. Phys., 11, 13325–13337, doi:10.5194/acp-11-13325-2011, 2011.

Hilton, F., Armante, R., August, T., Barnet, C., Bouchard, A., Camy-Peyret, C., Capelle, V., Clarisse, L., Clerbaux, C., Coheur, P.-., Collard, A., Crevoisier, C., Dufour, G., Edwards, D., Faijan, F., Fourrié, N., Gambacorta, A., Goldberg, M., Guidard, V., Hurtmans, D., Illingworth, S., Jacquinet-Husson, N., Kerzenmacher, T., Klaes, D., Lavanant, L., Masiello, G., Matricardi, M., McNally, A., Newman, S., Pavelin, E., Payan, S., Péquignot, E., Peyridieu, S., Phulpin, T., Remedios, J., Schlüssel, P., Serio, C., Strow, L., Stubenrauch, C., Taylor, J., Tobin, D., Wolf, W., and Zhou, D.: Hyperspectral earth observation from IASI, B. Am. Meteorol. Soc., 93, 347–370, 2012.

Hornbrook, R. S., Blake, D. R., Diskin, G. S., Fried, A., Fuelberg, H. E., Meinardi, S., Mikoviny, T., Richter, D., Sachse, G. W., Vay, S. A., Walega, J., Weibring, P., Weinheimer, A. J., Wiedinmyer, C., Wisthaler, A., Hills, A., Riemer, D. D., and Apel, E. C.: Observations of nonmethane organic compounds during ARCTAS – Part 1: Biomass burning emissions and plume enhancements, Atmos. Chem. Phys., 11, 11103–11130, doi:10.5194/acp-11-11103-2011, 2011.

Inness, A., Baier, F., Benedetti, A., Bouarar, I., Chabrillat, S., Clark, H., Clerbaux, C., Coheur, P., Engelen, R. J., Errera, Q., Flemming, J., George, M., Granier, C., Hadji-Lazaro, J., Huijnen, V., Hurtmans, D., Jones, L., Kaiser, J. W., Kapsomenakis, J., Lefever, K., Leitão, J., Razinger, M., Richter, A., Schultz, M. G., Simmons, A. J., Suttie, M., Stein, O., Thépaut, J.-N., Thouret, V., Vrekoussis, M., Zerefos, C., and the MACC team: The MACC reanalysis: an 8 yr data set of atmospheric composition, Atmos. Chem. Phys., 13, 4073–4109, doi:10.5194/acp-13-4073-2013, 2013.

Jacob, D. J., Crawford, J. H., Maring, H., Clarke, A. D., Dibb, J. E., Emmons, L. K., Ferrare, R. A., Hostetler, C. A., Russell, P. B., Singh, H. B., Thompson, A. M., Shaw, G. E., McCauley, E., Pederson, J. R., and Fisher, J. A.: The Arctic Research of the Composition of the Troposphere from Aircraft and Satellites (ARCTAS) mission: design, execution, and first results, Atmos. Chem. Phys., 10, 5191–5212, doi:10.5194/acp-10-5191-2010, 2010.

Title Page

Abstract | Introduction

Conclusions | References

Tables | Figures

|◄ | ►|

◄ | ►

Back | Close

Full Screen / Esc

Printer-friendly Version

Interactive Discussion

Jaffe, D., Bertschi, I., Jaegle, L., Novelli, P., Reid, J. S., Tanimoto, H., Vingarzan, R., and Westphal, D. L.: Long-range transport of Siberian biomass burning emissions and impact on surface ozone in western North America, Geophys. Res. Lett., 31, L16106, doi:10.1029/2004gl020093, 2004.

5   Jaffe, D. A. and Wigder, N. L.: Ozone production from wildfires: A critical review, Atmos. Environ., 51, 1–10, doi:10.1016/j.atmosenv.2011.11.063, 2012.

Jones, A. R., Thomson, D. J., Hort, M., and Devenish, B.: The UK Met Office's next-generation atmospheric dispersion model, NAME III, in: Air Pollution Modeling and its Application XVII (Proceedings of the 27th NATO/CCMS International Technical Meeting on Air Pollution Mod-

10   elling and its Application), edited by: Borrego, C. and Norman, A.-L., Springer, 580–589, 2007.

Kerzenmacher, T., Dils, B., Kumps, N., Blumenstock, T., Clerbaux, C., Coheur, P.-F., Demoulin, P., García, O., George, M., Griffith, D. W. T., Hase, F., Hadji-Lazaro, J., Hurtmans, D., Jones, N., Mahieu, E., Notholt, J., Paton-Walsh, C., Raffalski, U., Ridder, T., Schneider, M.,

15   Servais, C., and De Mazière, M.: Validation of IASI FORLI carbon monoxide retrievals using FTIR data from NDACC, Atmos. Meas. Tech., 5, 2751–2761, doi:10.5194/amt-5-2751-2012, 2012.

Langenfelds, R. L., Francey, R. J., Pak, B. C., Steele, L. P., Lloyd, J., Trudinger, C. M., and Allison, C. E.: Interannual growth rate variations of atmospheric CO_2 and its $\delta^{13}C$, H_2, CH_4,

20   and CO between 1992 and 1999 linked to biomass burning, Global Biogeochem. Cy., 16, 1048, doi:10.1029/2001gb001466, 2002.

Le Breton, M., Bacak, A., Muller, J. B. A., O'Shea, S. J., Xiao, P., Ashfold, M. N. R., Cooke, M. C., Batt, R., Shallcross, D. E., Oram, D. E., Forster, G., Bauguitte, S. J.-B., and Percival, C. J.: Airborne hydrogen cyanide measurements using a chemical ionisation mass spectrometer

25   for the plume identification of biomass burning forest fires, Atmos. Chem. Phys. Discuss., 13, 5649–5685, doi:10.5194/acpd-13-5649-2013, 2013.

LeCanut, P., Andreae, M. O., Harris, G. W., Wienhold, F. G., and Zenker, T.: Airborne studies of emissions from savanna fires in southern Africa, 1. Aerosol emissions measured with a laser optical particle counter, J. Geophys. Res.-Atmos., 101, 23615–23630,

30   doi:10.1029/95jd02610, 1996.

Lewis, A. C., Evans, M. J., Hopkins, J. R., Punjabi, S., Read, K. A., Purvis, R. M., Andrews, S. J., Moller, S. J., Carpenter, L. J., Lee, J. D., Rickard, A. R., Palmer, P. I., and Parrington, M.: The

Title Page

Abstract | Introduction

Conclusions | References

Tables | Figures

|◄ | ►|

◄ | ►

Back | Close

Full Screen / Esc

Printer-friendly Version

Interactive Discussion

influence of biomass burning on the global distribution of selected non-methane organic compounds, Atmos. Chem. Phys., 13, 851–867, doi:10.5194/acp-13-851-2013, 2013.

Li, Q. B., Jacob, D. J., Yantosca, R. M., Heald, C. L., Singh, H. B., Koike, M., Zhao, Y. J., Sachse, G. W., and Streets, D. G.: A global three-dimensional model analysis of the atmospheric budgets of HCN and CH_3CN: constraints from aircraft and ground measurements, J. Geophys. Res.-Atmos., 108, 8827, doi:10.1029/2002jd003075, 2003.

Marquis, M. and Tans, P.: Climate change – carbon crucible, Science, 320, 460–461, doi:10.1126/science.1156451, 2008.

McMillan, A. M. S., Goulden, M. L., and Tyler, S. C.: Stoichiometry of CH_4 and CO_2 flux in a California rice paddy, J. Geophys. Res.-Biogeo., 112, G01008, doi:10.1029/2006jg000198, 2007.

Monks, P. S., Granier, C., Fuzzi, S., Stohl, A., Williams, M. L., Akimoto, H., Amann, M., Baklanov, A., Baltensperger, U., Bey, I., Blake, N., Blake, R. S., Carslaw, K., Cooper, O. R., Dentener, F., Fowler, D., Fragkou, E., Frost, G. J., Generoso, S., Ginoux, P., Grewe, V., Guenther, A., Hansson, H. C., Henne, S., Hjorth, J., Hofzumahaus, A., Huntrieser, H., Isaksen, I. S. A., Jenkin, M. E., Kaiser, J., Kanakidou, M., Klimont, Z., Kulmala, M., Laj, P., Lawrence, M. G., Lee, J. D., Liousse, C., Maione, M., McFiggans, G., Metzger, A., Mieville, A., Moussiopoulos, N., Orlando, J. J., O'Dowd, C. D., Palmer, P. I., Parrish, D. D., Petzold, A., Platt, U., Poeschl, U., Prevot, A. S. H., Reeves, C. E., Reimann, S., Rudich, Y., Sellegri, K., Steinbrecher, R., Simpson, D., ten Brink, H., Theloke, J., van der Werf, G. R., Vautard, R., Vestreng, V., Vlachokostas, C., and von Glasow, R.: Atmospheric composition change – global and regional air quality, Atmos. Environ., 43, 5268–5350, doi:10.1016/j.atmosenv.2009.08.021, 2009.

Murphy, J. G., Oram, D. E., and Reeves, C. E.: Measurements of volatile organic compounds over West Africa, Atmos. Chem. Phys., 10, 5281–5294, doi:10.5194/acp-10-5281-2010, 2010.

O'Shea, S. J., Bauguitte, S. J.-B., Gallagher, M. W., Lowry, D., and Percival, C. J.: Development of a cavity-enhanced absorption spectrometer for airborne measurements of CH_4 and CO_2, Atmos. Meas. Tech., 6, 1095–1109, doi:10.5194/amt-6-1095-2013, 2013.

Palmer, P. I., Parrington, M., Lee, J. D., Lewis, A. C., Rickard, A. R., Bernath, P. F., Duck, T. J., Waugh, D. L., Tarasick, D. W., Andrews, S., Aruffo, E., Bailey, L. J., Barrett, E., Bauguitte, S. J.-B., Curry, K. R., Di Carlo, P., Chisholm, L., Dan, L., Forster, G., Franklin, J. E., Gibson, M. D., Griffin, D., Helmig, D., Hopkins, J. R., Hopper, J. T., Jenkin, M. E., Kindred, D.,

S. J. O'Shea et al.

Title Page

Abstract | Introduction

Conclusions | References

Tables | Figures

|◀ | ▶|

◀ | ▶

Back | Close

Full Screen / Esc

Printer-friendly Version

Interactive Discussion

Kliever, J., Le Breton, M., Matthiesen, S., Maurice, M., Moller, S., Moore, D. P., Oram, D. E., O'Shea, S. J., Christopher Owen, R., Pagniello, C. M. L. S., Pawson, S., Percival, C. J., Pierce, J. R., Punjabi, S., Purvis, R. M., Remedios, J. J., Rotermund, K. M., Sakamoto, K. M., da Silva, A. M., Strawbridge, K. B., Strong, K., Taylor, J., Trigwell, R., Tereszchuk, K. A., Walker, K. A., Weaver, D., Whaley, C., and Young, J. C.: Quantifying the impact of BOReal forest fires on Tropospheric oxidants over the Atlantic using Aircraft and Satellites (BORTAS) experiment: design, execution and science overview, Atmos. Chem. Phys. Discuss., 13, 4127–4181, doi:10.5194/acpd-13-4127-2013, 2013.

Parrington, M., Palmer, P. I., Lewis, A. C., Lee, J. D., Rickard, A. R., Di Carlo, P., Taylor, J. W., Hopkins, J. R., Punjabi, S., Oram, D. E., Forster, G., Aruffo, E., Moller, S. J., Bauguitte, S. J.-B., Allan, J. D., Coe, H., and Leigh, R. J.: Ozone photochemistry in boreal biomass burning plumes, Atmos. Chem. Phys. Discuss., 13, 1795–1853, doi:10.5194/acpd-13-1795-2013, 2013.

Pickett-Heaps, C. A., Jacob, D. J., Wecht, K. J., Kort, E. A., Wofsy, S. C., Diskin, G. S., Worthy, D. E. J., Kaplan, J. O., Bey, I., and Drevet, J.: Magnitude and seasonality of wetland methane emissions from the Hudson Bay Lowlands (Canada), Atmos. Chem. Phys., 11, 3773–3779, doi:10.5194/acp-11-3773-2011, 2011.

Seiler, W. and Crutzen, P. J.: Estimates of gross and net fluxes of carbon between the biosphere and the atmosphere from biomass burning, Climatic Change, 2, 207–247, doi:10.1007/bf00137988, 1980.

Simpson, I. J., Rowland, F. S., Meinardi, S., and Blake, D. R.: Influence of biomass burning during recent fluctuations in the slow growth of global tropospheric methane, Geophys. Res. Lett., 33, L22808, doi:0.1029/2006gl027330, 2006.

Simpson, I. J., Akagi, S. K., Barletta, B., Blake, N. J., Choi, Y., Diskin, G. S., Fried, A., Fuelberg, H. E., Meinardi, S., Rowland, F. S., Vay, S. A., Weinheimer, A. J., Wennberg, P. O., Wiebring, P., Wisthaler, A., Yang, M., Yokelson, R. J., and Blake, D. R.: Boreal forest fire emissions in fresh Canadian smoke plumes: C_1-C_{10} volatile organic compounds (VOCs), CO_2, CO, NO_2, NO, HCN and CH_3CN, Atmos. Chem. Phys., 11, 6445–6463, doi:10.5194/acp-11-6445-2011, 2011.

Simpson, I. J., Sulbaek Andersen, M. P., Meinardi, S., Bruhwiler, L., Blake, N. J., Helmig, D., Rowland, F. S., and Blake, D. R.: Long-term decline of global atmospheric ethane concentrations and implications for methane, Nature, 488, 490–494, doi:10.1038/nature11342, 2012.

Title Page

Abstract | Introduction

Conclusions | References

Tables | Figures

|◄ | ►|

◄ | ►

Back | Close

Full Screen / Esc

Printer-friendly Version

Interactive Discussion

Singh, H. B., Salas, L., Herlth, D., Kolyer, R., Czech, E., Viezee, W., Li, Q., Jacob, D. J., Blake, D., Sachse, G., Harward, C. N., Fuelberg, H., Kiley, C. M., Zhao, Y., and Kondo, Y.: In situ measurements of HCN and CH_3CN over the Pacific Ocean: Sources, sinks, and budgets, J. Geophys. Res.-Atmos., 108, 8795, doi:10.1029/2002jd003006, 2003.

Singh, H. B., Anderson, B. E., Brune, W. H., Cai, C., Cohen, R. C., Crawford, J. H., Cubison, M. J., Czech, E. P., Emmons, L., Fuelberg, H. E., Huey, G., Jacob, D. J., Jimenez, J. L., Kaduwela, A., Kondo, Y., Mao, J., Olson, J. R., Sachse, G. W., Vay, S. A., Weinheimer, A., Wennberg, P. O., Wisthaler, A., and the ARCTAS Science Team: Pollution influences on atmospheric composition and chemistry at high northern latitudes: boreal and California forest fire emissions, Atmos. Environ., 44, 4553–4564, doi:10.1016/j.atmosenv.2010.08.026, 2010.

Susott, R. A., Olbu, G. J., Baker, S. P., Ward, D. E., Kauffman, J. B., and Shea, R.: Carbon, hydrogen, nitrogen, and thermogravimetric analysis of tropical ecosystem biomass, in: Biomass Burning and Global Change, edited by: Levine, J. S., MIT Press, Cambridge, 350–360, 1996.

van der Werf, G. R., Randerson, J. T., Giglio, L., Collatz, G. J., Mu, M., Kasibhatla, P. S., Morton, D. C., DeFries, R. S., Jin, Y., and van Leeuwen, T. T.: Global fire emissions and the contribution of deforestation, savanna, forest, agricultural, and peat fires (1997–2009), Atmos. Chem. Phys., 10, 11707–11735, doi:10.5194/acp-10-11707-2010, 2010.

van Leeuwen, T. T. and van der Werf, G. R.: Spatial and temporal variability in the ratio of trace gases emitted from biomass burning, Atmos. Chem. Phys., 11, 3611–3629, doi:10.5194/acp-11-3611-2011, 2011.

Vay, S. A., Choi, Y., Vadrevu, K. P., Blake, D. R., Tyler, S. C., Wisthaler, A., Hecobian, A., Kondo, Y., Diskin, G. S., Sachse, G. W., Woo, J. H., Weinheimer, A. J., Burkhart, J. F., Stohl, A., and Wennberg, P. O.: Patterns of CO_2 and radiocarbon across high northern latitudes during International Polar Year 2008, J. Geophys. Res.-Atmos., 116, D14301, doi:10.1029/2011jd015643, 2011.

WDCGG: WMO World Data Centre for Greenhouse Gases, Japan Meteorological Agency, Tokyo, available at: http://ds.data.jma.go.jp/gmd/wdcgg/wdcgg.html, last access: 22 February 2013, 2013.

Wofsy, S. C., Fan, S. M., Blake, D. R., Bradshaw, J. D., Sandholm, S. T., Singh, H. B., Sachse, G. W., and Harriss, R. C.: Factors influencing atmospheric composition over sub-arctic North-America during summer, J. Geophys. Res.-Atmos., 99, 1887–1897, doi:10.1029/93jd02256, 1994.

Wotawa, G. and Trainer, M.: The influence of Canadian forest fires on pollutant concentrations in the United States, Science, 288, 324–328, doi:10.1126/science.288.5464.324, 2000.

Wotton, B. M., Nock, C. A., and Flannigan, M. D.: Forest fire occurrence and climate change in Canada, Int. J. Wildland Fire, 19, 253–271, doi:10.1071/wf09002, 2010.

5   Witham, C. and Manning, A.: Impacts of Russian biomass burning on UK air quality', Atmos. Environ., 41, 37, 8075–8090, doi:10.1016/j.atmosenv.2007.06.058, 2007.

Yokelson, R. J., Griffith, D. W. T., and Ward, D. E.: Open-path Fourier transform infrared studies of large-scale laboratory biomass fires, J. Geophys. Res.-Atmos., 101, 21067–21080, doi:10.1029/96jd01800, 1996.

10   Yokelson, R. J., Goode, J. G., Ward, D. E., Susott, R. A., Babbitt, R. E., Wade, D. D., Bertschi, I., Griffith, D. W. T., and Hao, W. M.: Emissions of formaldehyde, acetic acid, methanol, and other trace gases from biomass fires in North Carolina measured by airborne Fourier transform infrared spectroscopy, J. Geophys. Res.-Atmos., 104, 30109–30125, doi:10.1029/1999jd900817, 1999.

Table 1. Statistics for all BORTAS flights excluding the transits from Cranfield, UK to Nova Scotia, Canada and the return journey.

	Mean	Median	Minimum	Maximum	BB plume mean	Background mean
CO_2, ppm	384.8	385.1	371.5	397.1	385.8	383.8
CH_4, ppb	1859	1857	1797	1968	1859	1859

Title Page

Abstract | Introduction

Conclusions | References

Tables | Figures

◀◀ | ▶▶

◀ | ▶

Back | Close

Full Screen / Esc

Printer-friendly Version

Interactive Discussion

Table 2. Emission ratios (ER), normalised excess mixing ratios (NEMR) and emission factors (EF) determined by sampling boreal biomass burning plumes over Eastern Canada. MCE is the modified combustion efficiency, a measure of the combustion phase of the fire. The ER and EF determined in this study show good agreement with previous studies in boreal regions. Andreae and Merlet (2012) and Akagi et al. (2011) have compiled values from the literature for extra tropical forests. Simpson et al. (2011) report values for forest fires in boreal Canada made as part of the ARCTAS project. Units are (mol (mol CO)$^{-1}$) for the NEMR/ERs and g (kg dry matter)$^{-1}$ for the EFs.

	Flight	MCE	CO_2		CO		CH_4	
			ER/NEMR	EF	ER/NEMR	EF	ER/NEMR	EF
Fresh plume	B626	0.83 ± 0.01	5.1 ± 0.3	1512 ± 185	–	189 ± 23	0.079 ± 0.001	8.5 ± 0.9
Aged plumes (> 1 day)	B621 Run 3	0.90 ± 0.01	9.1 ± 0.8	1638 ± 255	–	114 ± 17	0.079 ± 0.004	5.2 ± 0.7
	B621 Run 15	–	–	–	–	–	0.109 ± 0.003	–
	B621 Profile 2	0.90 ± 0.001	9.4 ± 0.2	1648 ± 169	–	111 ± 11	0.05 ± 0.001	3.3 ± 0.3
	B621 Profile 3	–	–	–	–	–	0.16 ± 0.01	–
	B622 Run 1	0.89 ± 0.01	8.1 ± 0.5	1618 ± 216	–	126 ± 17	0.078 ± 0.003	5.7 ± 0.7
	B622 Run 3	0.93 ± 0.01	14.4 ± 0.2	1708 ± 173	–	75 ± 8	0.044 ± 0.001	1.8 ± 0.2
	B622 Run 6	0.92 ± 0.04	13 ± 7	1683 ± 1400	–	84 ± 73	0.12 ± 0.04	5.9 ± 3.9
	B622 Run 9	0.92 ± 0.03	12 ± 5	1679 ± 1000	–	87 ± 53	0.12 ± 0.05	6.1 ± 1
	B623 Run 1 and 2	–	–	–	–	–	0.133 ± 0.001	–
	B623 Run 3	–	–	–	–	–	0.093 ± 0.001	–
	B623 Run 5 and 6	0.93 ± 0.001	14.2 ± 0.2	1702 ± 173	–	76 ± 8	0.081 ± 0.001	3.5 ± 0.4
Literature values	Andreae and Merlet (2001)	–	–	1569 ± 131	–	107 ± 37	–	4.7 ± 1.9
	Simpson et al. (2011)	–	9.1 ± 5.8	1616 ± 180	–	113 ± 72	0.072 ± 0.044	4.7 ± 2.9
	Akagi et al. (2011)	–	–	1489 ± 121	–	127 ± 45	–	6.0 ± 3.1
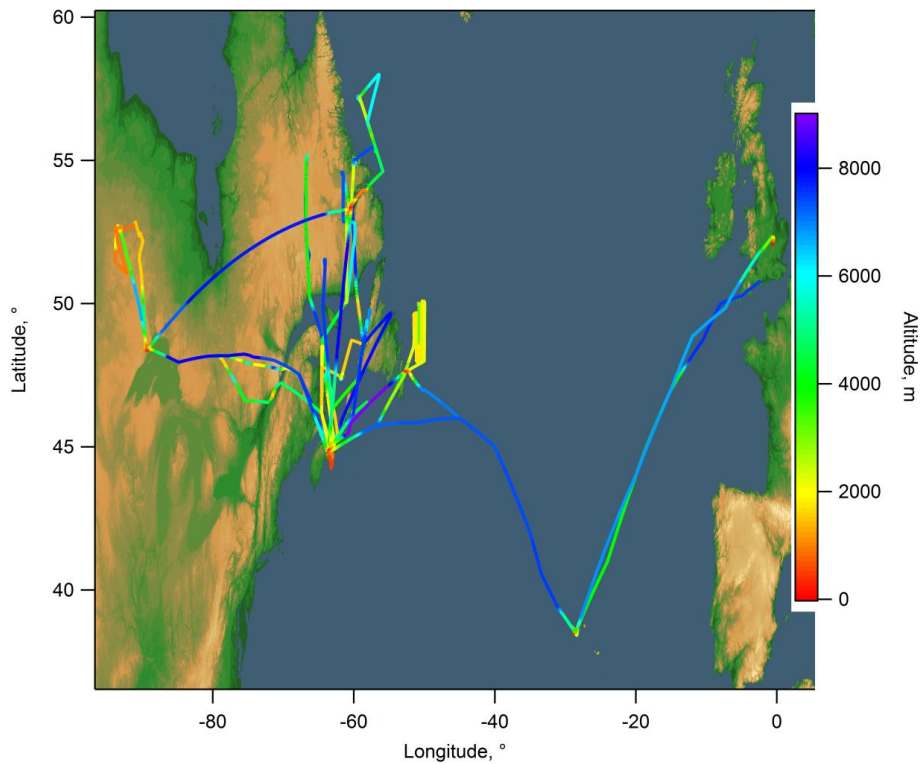
Fig. 1. The geographic coverage of flights during BORTAS, 12 July to 3 August 2011.
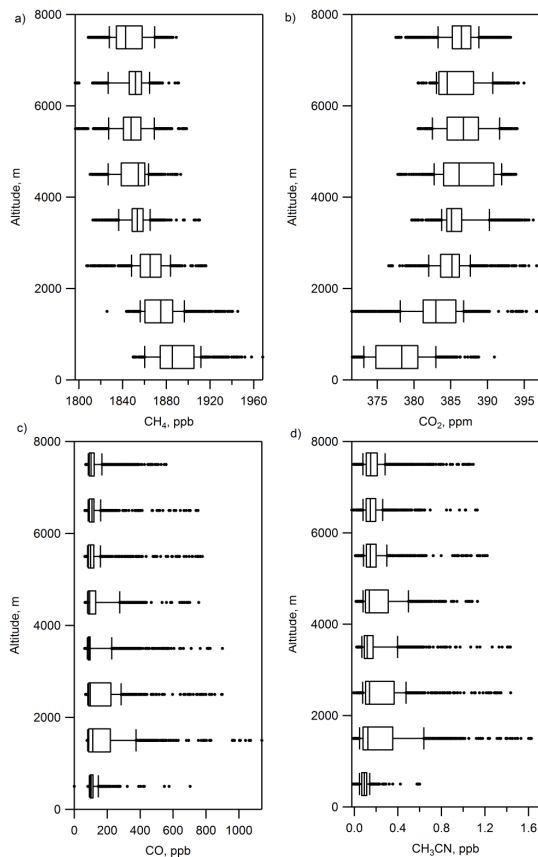
Printer-friendly Version

Interactive Discussion

Fig. 2. A summary of the observations of CH_4, CO_2, CO and CH_3CN made on the FAAM BAe-146 during the BORTAS project. The transits from Cranfield, UK to Nova Scotia, Canada and the return journey have been excluded from these plots. Boxes are 25th and 75th percentiles, whiskers are 10th and 90th percentiles and the markers are outliers.

Title Page

Abstract | Introduction

Conclusions | References

Tables | Figures

|◄ | ►|

◄ | ►

Back | Close

Full Screen / Esc

Printer-friendly Version

Interactive Discussion
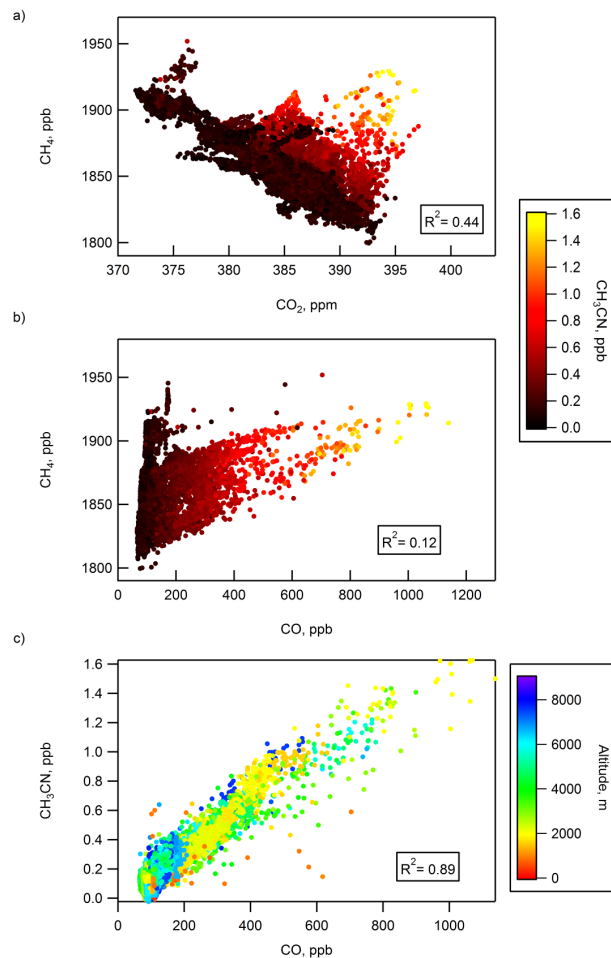
Fig. 3. The relationships between CH_4, CO_2, CO and CH_3CN for the BORTAS flights with the exception of the Atlantic transits.

Title Page

Abstract | Introduction

Conclusions | References

Tables | Figures

|◄ | ►|

◄ | ►

Back | Close

Full Screen / Esc

Printer-friendly Version

Interactive Discussion
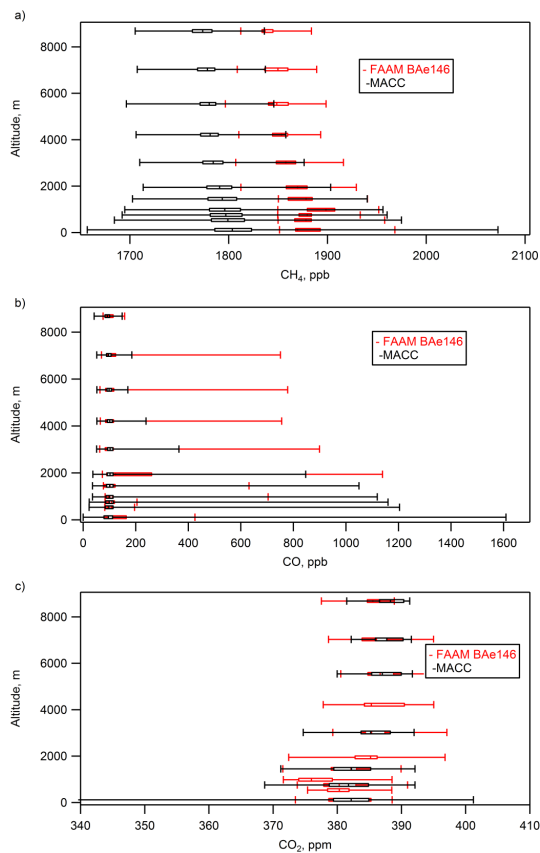
Fig. 4. Comparison between in situ measurements on the FAAM BAe-146 and those derived from the Monitoring Atmospheric Composition and Change (MACC) project over the BORTAS sampling domain and period.

Title Page

Abstract | Introduction

Conclusions | References

Tables | Figures

◀ | ▶|

◀ | ▶

Back | Close

Full Screen / Esc

Printer-friendly Version

Interactive Discussion
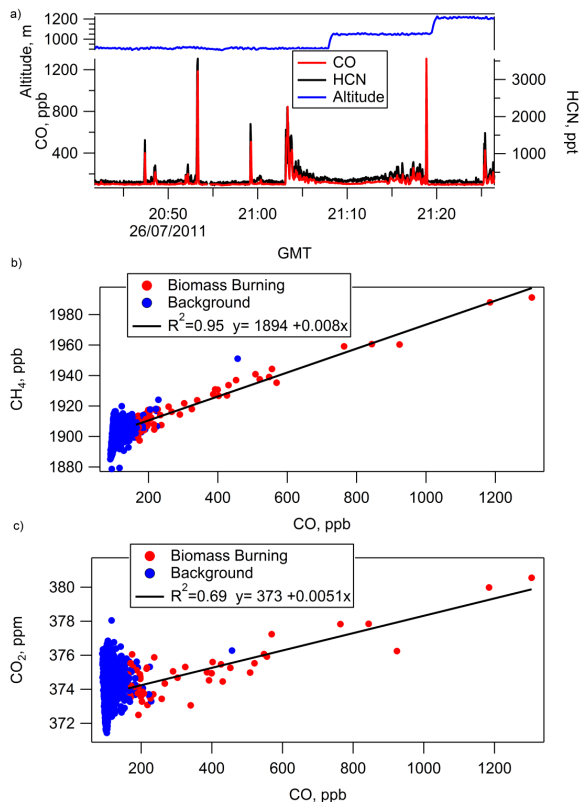
Fig. 5. (a) Time series of CO and HCN in fresh boreal biomass burning plumes measured by BORTAS flight B626 over Northwest Ontario. BB plumes were identified using simultaneous measurements of tracer species CO and HCN (the thresholds used were the periods during which CO and HCN were both 6 standard deviations greater than their local background). Strong linear relationships were found for both **(b)** CH_4 and **(c)** CO_2 with CO for measurements made within these plumes.
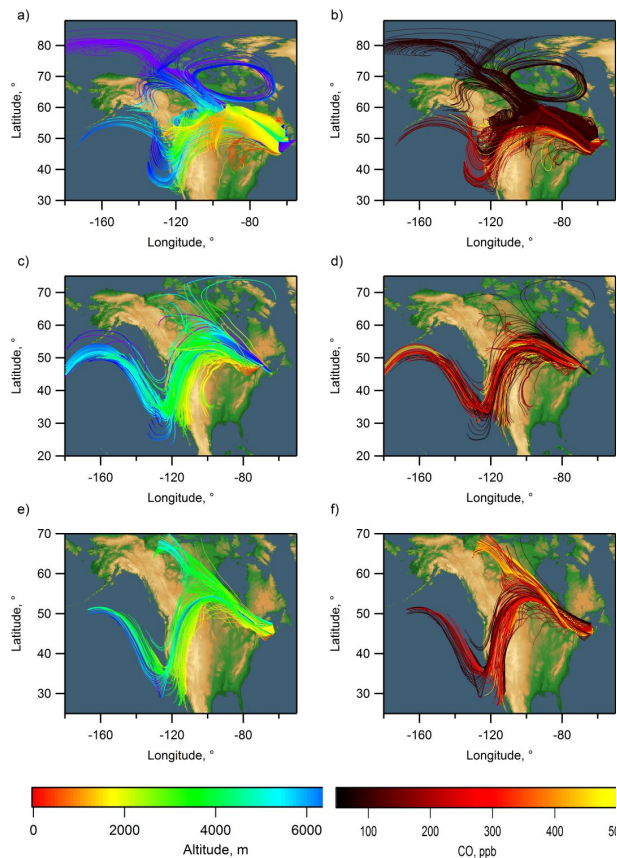
Fig. 6. Five day HYSPLIT back trajectories whose endpoints co-locate with every minute of the FAAM BAe-146 flight track, for flights B621 (**a**, **b**), B622 (**c**, **d**) and B623 (**e** and **f**). Plots **(a)**, **(c)** and **(e)** have been colour coded by altitude, while **(b)**, **(d)** and **(f)** have been colour coded by the CO measurement on the FAAM BAe-146 at the endpoint of each trajectory.
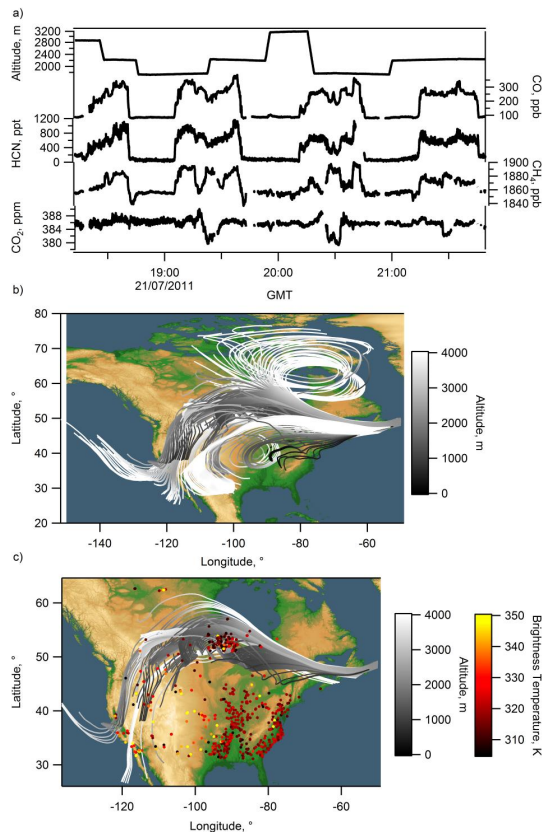
Fig. 7. (a) Time series whilst sampling a biomass burning plume near the coast of Newfoundland during flight B624. **(b)** HYSPLIT 5 day back trajectories for the whole of flight B624. The trajectories were started at 60 s intervals along the flight starting point. **(c)** Only the back trajectories that end whilst flying in a biomass burning plume, as identified by the in situ HCN and CO measurements on the FAAM BAe-146. Markers are active fires detected by MODIS for the previous 5 days to the flight.
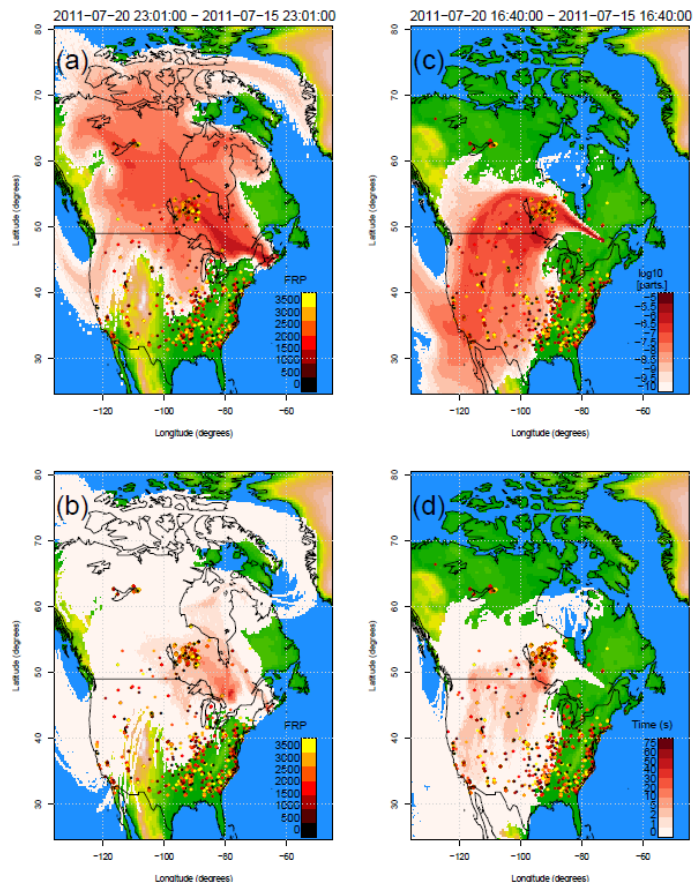
Fig. 8. NAME total column (**a** and **c**) and surface (**b** and **d**) sensitivity footprints for two BB plumes sampled during flight B623 (**a** and **b**) and B622 (**c** and **d**). Darker shading represents a greater sensitivity to that region. Markers are active fires detected by MODIS for the previous 5 days to the flight and they are coloured by the fire radiative power (FRP).

Title Page

Abstract | Introduction

Conclusions | References

Tables | Figures

|◄ | ►|

◄ | ►

Back | Close
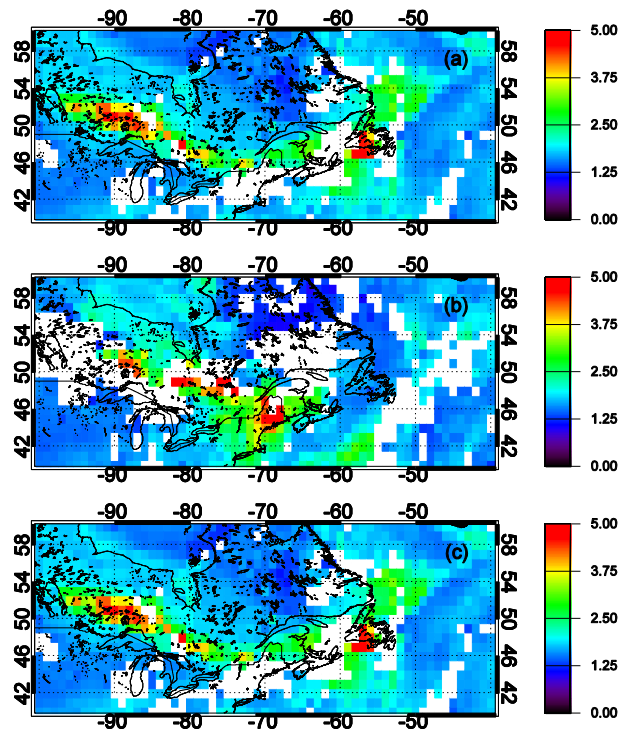
Full Screen / Esc

Fig. 9. The daytime mean total column CO (1×10^{18} mol cm^{-2}) on a 1° by 1° grid from the Infrared Atmospheric Sounding Interferometer (IASI) on the MetOp-A satellite for the dates **(a)** 18 July 1011, **(b)** 20 July 2011 and **(c)** 21 July 2011.
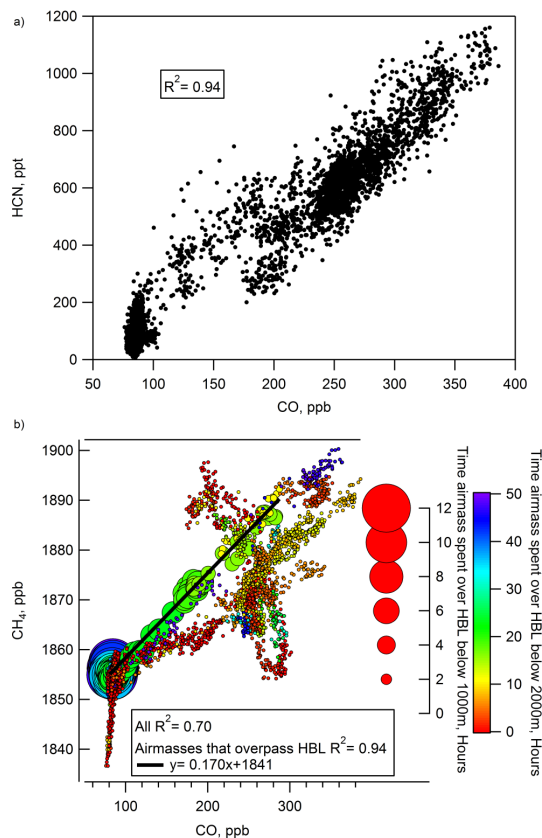
Fig. 10. Tracer-tracer relationships for a BB plume sampled during flight B624. Plot **(b)** showing the relationship between CH_4 and CO, has been colour coded and sized according to the length of time the HYSPLIT trajectories spent over wetlands near Hudson Bay (HBL).

Title Page

Abstract | Introduction

Conclusions | References

Tables | Figures

|◄ | ►|

◄ | ►

Back | Close

Full Screen / Esc

Printer-friendly Version

Interactive Discussion